Cyclic Prefix Based Universal Filtered Multi-carrier System and Performance Analysis

Lei Zhang, Pei Xiao and Atta Quddus

***Abstract*—Recently proposed universal filtered multi-carrier (UFMC) system is not an orthogonal system in multipath channel environments and might cause significant performance loss. In this paper, we propose a cyclic prefix (CP) based UFMC system and first analyze the conditions for interference-free one-tap equalization in the absence of transceiver imperfections. Then the corresponding signal model and output SNR (signal-to-noise ratio) expression are derived. In the presence of carrier frequency offset (CFO), timing offset (TO) and insufficient CP length, we establish an analytical system model as a summation of desired signal, inter-symbol interference (ISI), inter-carrier interference (ICI) and noise. New channel equalization algorithms are proposed based on the derived analytical signal model. Numerical results show that the derived model matches the simulation results precisely, and the proposed equalization algorithms improve the UFMC system performance in terms of bit error rate (BER).**

I. Introduction

Universal filtered multi-carrier (UFMC) systems offer a flexibility of filtering subbands consisting of arbitrary number of consecutive subcarriers to suppress out of band (OoB) emission, while keeping the orthogonality between subbands and subcarriers in one subband [1], [2], [3], [4]. Comparing to other candidate waveforms for the next generation wireless communication systems, it employs low complexity one-tap channel equalization similar to the orthogonal frequency division multiplexing (OFDM) system but offers much lower OoB emission. Note that filter-bank multi-carrier (FBMC) system [5], [6] can provide even lower OoB emission than UFMC system, and the recently proposed cyclic prefix (CP) FBMC can also achieve interference-free one-tap channel equalization [7]. However, comparing with the FBMC system, the UFMC system inherits the advantageous properties of OFDM systems, e.g., ease in the implementation of multi-antenna techniques and low complexity channel estimation and equalization algorithms. In addition, comparing with Filtered OFDM system that filters the whole bandwidth after OFDM modulation [8], the UFMC system provides *flexibility* to filter a subband with arbitrary bandwidth to enable the system adopted for specific users or service types by adjusting the subband and filter parameters only. For example, a UFMC system may serve two types of services (e.g., tactile and machine type communications [9]) in two subbands with different communications requirements and frame structure. The subband filter in UFMC enable the two services in different subbands to be designed independently without generating significant inter-service-band-interference (ISBI) [10]. Such flexibility makes the UFMC as one of the most promising candidate waveforms for 5G systems and beyond.

It should be pointed out that the original UFMC system as proposed in [1], [3] is no longer an orthogonal system in multipath environments since there is no guard interval between symbols. Although it has been claimed that the subband filter with a length comparable to that of the channel will incur negligible performance loss, this claim has not been proved analytically and may not be true for some scenarios (e.g., in harsh channel conditions). Alternatively, CP as an option can be added *after* the subband filtering to avoid the inter-symbol interference (ISI) [1]. However, the system can not achieve interference-free one-tap equalization as circular convolution property is destroyed. The conditions of how to achieve it and the analysis for the performance loss in non-ideal case are still open issues. Note that recently proposed filtered OFDM (f-OFDM) is also a CP based subband filtered OFDM technique [10]. However, f-OFDM system uses much longer FIR filter (e.g., half symbol duration) to process the subband signal and the filter tail extends to the adjacent OFDM symbols and also *overlap* each other in order to reduce the filter tail caused overhead. It unavoidably introduces ISI and the interference-free one-tap equalization does not hold.

In order to analyze the performance loss/gain and provide useful guideline for UFMC system design in practice, it is necessary to establish a mathematic framework by considering the carrier frequency offset (CFO), timing offset (TO), multipath channel and insufficient CP length. For CP-OFDM system, the insufficient CP length with CFO and TO is modeled in [11] and the optimal CP length for maximizing sum-rate are formulated in [12]. The performance of UFMC systems in the presence of CFO was analyzed in [13] and a filter was optimized to minimize the out of band leakage (OBL) in [14] by considering both CFO and TO. However, only single-path flat fading channel was considered in [13] and [14].

In this paper, we propose a new CP-UFMC system by adding CP *before* the subband filtering operation to achieve low complexity interference-free one-tap channel equalization in the absence of transceiver imperfections. Such a system has the same receiver implementation as the CP-OFDM system and therefore is *compatible to the legacy CP-OFDM system*. The applicability of one-tap equalization for CP-UFMC systems is examined, followed by the corresponding signal model and output SNR expression derivation. Next, the system model in the presence of CFO, TO and insufficient CP for the CP-UFMC is derived in terms of the desired signal, ISI and ICI (inter-carrier interference). In addition, new equalization algorithms are proposed to improve the system performance based on the derived model.

Notations: $\{\cdot\}^H$ and $\{\cdot\}^T$ stand for the Hermitian conjugate and transpose operation, respectively. We use $\mathcal{E}\{\mathbf{A}\}$ and trace$\{\mathbf{A}\}$ to denote the expectation and trace of matrix $\mathbf{A}$. $\mathbf{I}_M$ and $\mathbf{0}_{M\times N}$ refers to identity matrix of M dimension and $M \times N$ matrix with all of its elements being zero, respectively. We denote $*$ as a linear convolution operation of two vectors.

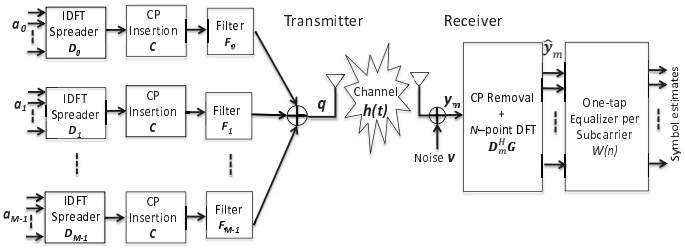

Fig. 1. Blocks diagrams for CP-UFMC transmitter and receiver.

II. CP-UFMC IN THE ABSENCE OF TRANSCEIVER IMPERFECTIONS

Let us assume a multi-carrier system that contains N subcarriers with its index set being $\mathcal{U} = [0, 1, \cdots, N-1]$. The N subcarriers are divided into M subbands with the k-th ($k = 0, 1, \cdots M-1$) subband comprising of N_k consecutive subcarriers from the set $\mathcal{U}$. The subcarrier index set for the k-th ($k = 1, \cdots M-1$) subband is $\mathcal{U}_k = [\sum_{i=0}^{k-1} N_i, \sum_{i=0}^{k-1} N_i + 1, \cdots, \sum_{i=0}^{k} N_i - 1]$ and $\mathcal{U}_0 = [0, 1, \cdots, N_0 - 1]$.

Assume the modulated symbols transmitting N subcarriers are $\mathbf{a} = [\mathbf{a}_0; \mathbf{a}_1; \cdots; \mathbf{a}_{M-1}] = [a(0), a(1), \cdots, a(N-1)]^T$, where $\mathbf{a}_k$ is a length N_k symbol vector transmitting on the k-th subband and consisting of elements $a(i)$ with $\mathcal{E}\{|a(i)|^2\} = \rho_{sym}^2$ for $i \in \mathcal{U}_k$. Let us assume the k-th subband filter is $\mathbf{f}_k = [f_k(0), f_k(1), \cdots, f_k(L_{F,k}-1)]$ with $L_{F,k}$ being the filter length. In order to have unified expressions for different subbands, let us define $L_{F,max} = \max(L_{F,k})$ for $k \in [0, 1, \cdots, M-1]$.

A. Proposed CP-UFMC System Model

As shown in Fig. 1, by adding CP and filtering the subband after IDFT (inverse discrete Fourier transform) operation, we can write the transmitting signal as

$$\mathbf{q} = \sum_{k=0}^{M-1} \frac{1}{\rho_k} \mathbf{f}_k * \mathbf{C}\mathbf{D}_k\mathbf{a}_k = \sum_{k=0}^{M-1} \frac{1}{\rho_k} \mathbf{F}_k\mathbf{C}\mathbf{D}_k\mathbf{a}_k \tag{1}$$

where $\mathbf{C} = [\mathbf{0}_{L_{CP}\times(N-L_{CP})}, \mathbf{I}_{L_{CP}}; \mathbf{I}_N]$ is the matrix form of the CP insertion operation with L_{CP} being the CP length and $L_{SYM} = N + L_{CP}$ being the symbol duration in UFMC samples. $\mathbf{F}_k \in \mathbb{C}^{L_{SYM}\times L_{SYM}}$ is a Toeplitz matrix with its first column being $\tilde{\mathbf{f}}_k = [f_k(0), f_k(1), \cdots, f_k(L_{F,k}-1), \mathbf{0}_{1\times(L_{SYM}-L_{F,k})}]^T \in \mathbb{C}^{L_{SYM}\times 1}$ and first row being $[f_k(0), \mathbf{0}_{1\times(L_{SYM}-1)}] \in \mathbb{C}^{1\times L_{SYM}}$. The dimension and structure of $\mathbf{F}_k$ implies that the filter tails are cut before the transmission. $\mathbf{D}_k \in \mathbb{C}^{N\times N_k}$ is the $(\sum_{i=0}^{k-1} N_i + 1)$-th to the $(\sum_{i=0}^{k} N_i)$-th columns of N-point normalized IDFT matrix $\mathbf{D}$. The i-th row and n-th column element of $\mathbf{D}$ is $d_{i,n} = \frac{1}{\sqrt{N}} e^{j2\pi in/N}$. $\rho_k = \sqrt{\frac{1}{N_k}\text{trace}(\mathbf{D}_k^H\mathbf{C}^H\mathbf{F}_k^H\mathbf{F}_k\mathbf{C}\mathbf{D}_k)}$ is the transmission power normalization factor of the k-th subband due to the CP insertion and filter tail cutting.

Let us assume the channel between the transmitter and the receiver at time t is $\mathbf{h}(t) = [h(0,t), h(1,t), \cdots, h(L_{CH}-1, t)]$ with L_{CH} being the channel length in number of samples. Without loss generality, we assume the overall channel gain $\sum_{i=0}^{L_{CH}-1} \mathcal{E}|h(i,t)|^2 = \rho_{CH}^2$. After CP removal and N-point DFT operation, the signal for the m-th subband at the receiver (before channel equalization) can be written as

$$\begin{aligned}\mathbf{y}_m &= \mathbf{D}_m^H\mathbf{G}[\mathbf{h}(t) * \mathbf{q}] + \mathbf{D}_m^H\mathbf{v} \\ &= \mathbf{D}_m^H\mathbf{G}\mathbf{H}(t) \sum_{k=0}^{M-1} \frac{1}{\rho_k}\mathbf{F}_k\mathbf{C}\mathbf{D}_k\mathbf{a}_k + \mathbf{y}_{ISI} + \mathbf{D}_m^H\mathbf{v}\end{aligned} \tag{2}$$

where $\mathbf{G} = [\mathbf{0}_{N\times L_{CP}}, \mathbf{I}_N]$ is matrix form of CP removal implementation. $\mathbf{H}(t) \in \mathbb{C}^{L_{SYM}\times L_{SYM}}$ is the equivalent channel convolution matrix of $\mathbf{h}(t)$. $\mathbf{v} = [v(0), v(1), \cdots, v(N-1)]^T$ is noise vector at the receiver and its i-th element $v(i)$ has a complex-valued Gaussian distribution $\mathcal{CN}(0, \sigma^2)$ with σ^2 being the noise variance and $\mathbf{y}_{ISI}$ is the ISI. In the ideal scenarios with sufficient CP length, $\mathbf{y}_{ISI} = \mathbf{0}$. When $L_{F,k} = 1$ (i.e., $\mathbf{F}_k = \mathbf{I}_{L_{SYM}}$), (2) boils down to CP-OFDM system.

The proposed transceiver diagram is shown in Fig. 1, and unlike the original UFMC system (where CP is an option can be added *after* subband filtering) [1], we add the CP *before* subband filtering. In addition, the proposed CP-UFMC system has exactly the same receiver implementation as CP-OFDM system, which avoids zero padding (and down-sampling) as well as high-order DFT operation as implemented in the original UFMC system [1], [2], [4].

B. Applicability for One-tap Equalization

We aim to achieve interference-free transmission by adding CP between UFMC symbols, we propose the following proposition:

Proposition 1: *Consider a CP-UFMC system that consists of N subcarriers with channel length and CP length being L_{CH} and L_{CP}. A sufficient condition to apply interference-free one-tap channel equalization to the m-th subband is:*

$$L_{CP} \geq L_{CH} + L_{F,m} - 2 \tag{3}$$

and in that case the signal model for the n-th subcarrier that belongs to the m-th subband is

$$z(n) = \frac{1}{\rho_m} H(n,t) F_m(n) a(n) + \hat{v}(n) \tag{4}$$

where $\hat{v}(n) = \sum_{l=0}^{N-1} \frac{1}{\sqrt{N}} e^{-j2\pi nl/N} v(l)$ is the noise after DFT operation. $H(n,t) = \sum_{l=0}^{N-1} e^{-j2\pi nl/N} h(l,t)$ and $F_m(n) = \sum_{l=0}^{N-1} e^{-j2\pi nl/N} f_m(l)$ are channel and filter frequency response at the n-th subcarrier.

Proof: In order to achieve ISI-free estimation (i.e., $\mathbf{y}_{ISI} = \mathbf{0}$), we have to set the CP length as: $L_{CP} \geq L_{CH} - 1$ and equation (3) is a sufficient condition since $L_{F,m} \geq 1$. Now let us focus on the conditions to achieve ICI-free system. When $L_{CP} \geq L_{CH} + L_{F,m} - 2$, we have $\mathbf{G}\mathbf{H}(t)\mathbf{F}_k\mathbf{C} = \mathbf{G}\mathbf{H}(t)\mathbf{C}\mathbf{G}\mathbf{F}_k\mathbf{C}$, substituting it into the first term (let us define it as $\mathbf{U}_m$) of equation (2) leads to $\mathbf{U}_m = \mathbf{D}_m^H\mathbf{G}\mathbf{H}(t)\mathbf{C}\sum_{k=0}^{M-1}\frac{1}{\rho_k}\mathbf{G}\mathbf{F}_k\mathbf{C}\mathbf{D}_k$. The interpretation of multiplying $\mathbf{G}$ and $\mathbf{C}$ in the left and right of matrix $\mathbf{H}(t)$ (similar for $\mathbf{F}_k$) is to reframe it to be a circulant matrix, i.e., $\mathbf{G}\mathbf{H}(t)\mathbf{C} = \mathbf{H}_{cir}(t)$ and $\mathbf{G}\mathbf{F}_k\mathbf{C} = \mathbf{F}_{cir,k}$, where $\mathbf{H}_{cir}(t)$ and $\mathbf{F}_{cir,k}$ are the circulant matrix of the channel vector $\bar{\mathbf{h}}(t) = [\mathbf{h}(t), \mathbf{0}_{1\times(L_{SYM}-L_{CH})}]^T$ and filter vector $\bar{\mathbf{f}}_k = [\mathbf{f}_k, \mathbf{0}_{1\times(L_{SYM}-L_{F,k})}]^T$, respectively. Rewriting $\mathbf{U}_m$ as $\mathbf{U}_m = \frac{1}{\rho_m}\mathbf{D}_m^H\mathbf{H}_{cir}(t)\mathbf{D}\mathbf{D}^H\mathbf{F}_{cir,m}\mathbf{D}_m + \mathbf{D}_m^H\mathbf{H}_{cir}(t)\mathbf{D}\sum_{k=0,k\neq m}^{M-1}\frac{1}{\rho_k}\mathbf{D}^H\mathbf{F}_{cir,k}\mathbf{D}_k$. Using the circular convolution property, we have $\mathbf{D}_m^H\mathbf{H}_{cir}(t)\mathbf{D} =$

$[\mathbf{0}_{N_m\times\sum_{i=0}^{m-1}N_i}, \mathbf{H}_{fd,m}, \mathbf{0}_{N_m\times(N-\sum_{i=0}^{m}N_i)}]$ and $\mathbf{D}^H\mathbf{F}_{cir,k}\mathbf{D}_k = [\mathbf{0}_{\sum_{i=0}^{k-1}N_i\times N_k}; \mathbf{F}_{fd,k}; \mathbf{0}_{(N-\sum_{i=0}^{k}N_i)\times N_k}]$, where the diagonal matrices $\mathbf{H}_{fd,m}(t) = \sqrt{N}\text{diag}[\mathbf{D}_m^H\bar{\mathbf{h}}(t)]$ and $\mathbf{F}_{fd,m} = \sqrt{N}\text{diag}(\mathbf{D}_m^H\bar{\mathbf{f}}_m)$. When $m = k$, we have $\mathbf{D}_m^H\mathbf{H}_{cir}(t)\mathbf{D}\mathbf{D}^H\mathbf{F}_{cir,m}\mathbf{D}_m = \mathbf{H}_{fd,m}(t)\mathbf{F}_{fd,m}$. When $m \neq k$, the non-zero parts of $\mathbf{D}_m^H\mathbf{H}_{cir}(t)\mathbf{D}$ and $\mathbf{D}^H\mathbf{F}_{cir,k}\mathbf{D}_k$ are not overlapped, leads to $\mathbf{D}_m^H\mathbf{H}_{cir}(t)\mathbf{D}\sum_{k=0,k\neq m}^{M-1}\frac{1}{\rho_k}\mathbf{D}^H\mathbf{F}_{cir,k}\mathbf{D}_k = \mathbf{0}$. Substitute them into $\mathbf{U}_m$ and noting the i-th row and k-th column element of $\mathbf{D}^H$ can be written as $d_{i,k} = \frac{1}{\sqrt{N}}e^{-j2\pi ik/N}$, we obtain (4).

Based on (4), we can derive the output SNR expectation of the n-th subcarrier that belongs to subband m as:

$$\mathcal{E}\{SNR(n)\} = \frac{\rho_{sym}^2}{\sigma^2}\cdot\rho_{CH}^2\cdot\frac{1}{\rho_m^2}\cdot|F_m(n)|^2 \quad (5)$$

When filter length $L_{F,m} = 1$, equation (5) converges to CP-OFDM system with sufficient CP length, i.e., $\mathcal{E}\{SNR^{ofdm}\} = \frac{N}{L_{SYM}}\cdot\frac{\rho_{sym}^2}{\sigma^2}\cdot\rho_{CH}^2$.

III. UFMC in the presence of CFO, TO and insufficient CP length

Due to the transceiver imperfections, it is more realistic to assume a certain level of CFO and TO present in the system. In addition, sufficient CP length is not always (and sometimes unnecessarily) satisfied in order to save system overhead. In this section, we will first derive an analytical model by taking all of the listed imperfection factors into consideration. Then new one-tap equalization algorithms are proposed to improve system performance in non-ideal cases.

1) Signal model in the presence of CFO, TO and insufficient CP length: Suppose the normalized (by subcarrier spacing Δf) CFO of m-th subband is ϵ_m, then we can rewrite $\mathbf{q}$ in (1) as

$$q(l)=\sum_{m=0}^{M-1}\sum_{i=0}^{L_{SYM}-1}\sum_{n\in\mathcal{U}_m}e^{j2\pi(i-L_{CP})(n+\epsilon_m)/N}f_m(l-i)a(n) \quad (6)$$

where $l = 0, 1, \cdots, L_{SYM}-1$. By considering the normalized (by UFMC sample duration: $\Delta T/N$ with ΔT being the symbol duration) synchronization error (e.g., TO) τ in the receiver, the received signal can be expressed as

$$\hat{y}(r) =\sum_{e=-\infty}^{\infty}\sum_{l=0}^{L_{SYM}-1}q(l)h_k(r-l-eL_{SYM}+\tau_t, r+\tau_t) \quad (7)$$

where $r = 0, 1, \cdots, L_{SYM}-1$ and $\tau_t = \tau + L_{CP}$.

Removing CP and performing N-point DFT on $\hat{y}(r)$, then

$$x_k(d)=\sum_{r=0}^{N-1}\hat{y}(r+L_{CP})e^{\frac{-j2\pi d(r+L_{CP})}{N}}+v_{os,k}(d) \quad (8)$$

2) Performance analysis: Since the modulated symbols $a(l)$ is uncorrelated to $a(k)$ if $l \neq k$ for $\forall l, \forall k \in \mathcal{U}$. In addition, signals from different UFMC symbols are also uncorrelated, by also noticing $\mathcal{E}|a(n)|^2 = \rho_{sym}^2$, we can express the power of desired signal, ISI, ICI and noise of the n-th subcarrier as

$$P(n) = P_D(n) + P_{ICI}(n) + P_{ISI}(n) + \sigma^2 \quad (9)$$

where

$$\begin{aligned} P_D(n) &= \rho_{sym}^2\mathcal{E}|\beta(n,n,0)|^2 \\ P_{ICI}(n) &= \rho_{sym}^2\sum_{t\in\mathcal{U}_m,t\neq n}\mathcal{E}|\beta(n,t,0)|^2 \\ P_{ISI}(n) &= \rho_{sym}^2\sum_{e=-\infty,e\neq0}^{\infty}\sum_{t\in\mathcal{U}_m}\mathcal{E}|\beta(n,t,e)|^2 \end{aligned} \quad (10)$$

$$\beta(n,t,e) = \sum_{r=0}^{N-1}\sum_{l=0}^{L_{SYM}-1}\sum_{m=0}^{M-1}\sum_{i=0}^{L_{SYM}-1}e^{\frac{j2\pi(i-L_{CP})(n+\epsilon_m)}{N}} e^{\frac{-j2\pi(r+L_{CP})t}{N}}h(r-l-eL_{SYM}+\tau_t, r+\tau_t)f_m(l-i) \quad (11)$$

To simplify the derivation of $|\beta(n,t,e)|^2$, let us define $T_m(l_1,l_2) = B_m(l_1)B_m^*(l_2)$ with $B_m(l_1) = \sum_{i=0}^{L_{SYM}-1}e^{\frac{j2\pi(i-L_{CP})(n+\epsilon_m)}{N}}f_m(l-i)$. For the FIR channel, we assume $\mathcal{E}\{h(l_1,t_1)h^*(l_2,t_2)\} = 0$ for $l_1 \neq l_2$ and $\mathcal{E}\{h(l_1,t_1)h^*(l_2,t_2)\} = R(l_1,t_1-t_2)$ for $l_1 = l_2$, with $R(l_1,t_1-t_2)$ being the autocorrelation function of the channel $\mathbf{h}(t)$ at the l_1-th path and l_2-th path at time t_1 and t_2. Using the equation and the definition of $T_m(l_1,l_2)$, we have

$$\begin{aligned} \mathcal{E}|\beta(n,t,e)|^2 = &\sum_{l_1=0}^{L_{SYM}-1}\sum_{l_2=0}^{l_1}\sum_{m=0}^{M-1}T_m(l_1,l_2)\sum_{r=l_1-l_2}^{N-1} \\ &e^{\frac{-j2\pi t(l_1-l_2)}{N}}R(r-l_1+\tau_t, l_1-l_2) \\ &+\sum_{l_1=0}^{L_{SYM}-1}\sum_{l_2=l_1}^{L_{SYM}-1}\sum_{m=0}^{M-1}T_m(l_1,l_2)\sum_{r=l_1-l_2}^{N-1-(l_2-l_1)} \\ &e^{\frac{-j2\pi t(l_1-l_2)}{N}}R(r-l_1+\tau_t, l_1-l_2) \end{aligned} \quad (12)$$

In the presence of interference, the SINR of the n-th subcarrier can be written as

$$SINR(n) = P_D(n)/[P_{ICI}(n)+P_{ISI}(n)+\sigma^2] \quad (13)$$

3) Proposed channel equalization algorithm: Based on the derived signal model in (9), (10) and (12) in the presence of CFO, TO and insufficient CP length, we propose linear one-tap channel equalization algorithms under the criteria of ZF (zero-forcing) and MMSE (minimum mean square error) as

$$W(n) = \frac{\beta(n,n,0)^H}{|\beta(n,n,0)|^2+\nu[P_{ICI}(n)+P_{ISI}(n)+\sigma^2]/\rho_{sym}^2} \quad (14)$$

where $\nu = 0$ for ZF algorithm and $\nu = 1$ for MMSE algorithm.

IV. Numerical results

We adopt LTE (Long Term Evolution) radio frame structure with total number of subcarriers $N = 2048$, subcarrier spacing $\Delta f = 15$ KHz and the symbol duration $\Delta T = 1/15000$ s. Without loss of generality, we assume that only the middle 120 subcarriers are occupied and they are divided into $M = 10$ equal bandwidth subbands. We adopt a finite impulse response (FIR) Chebyshev filter with OoB emission level equals to -50 dB and the filter length $L_{F,m} = 120$ taps. The LTE ETU (Extended Typical Urban) channel model is used and the CP length for OFDM system and UFMC system are 160 and 40, respectively, which leads to the two systems having the same overhead. The signal is modulated by 16-QAM (Quadrature

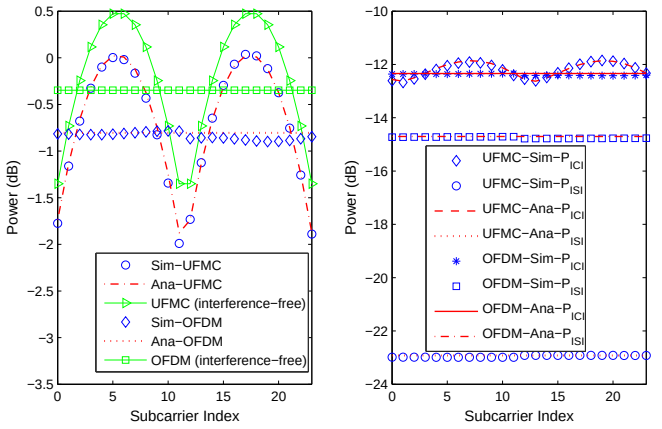

Fig. 2. Desired signal power, ICI and ISI at different subcarrier in both interference-free and interference cases.

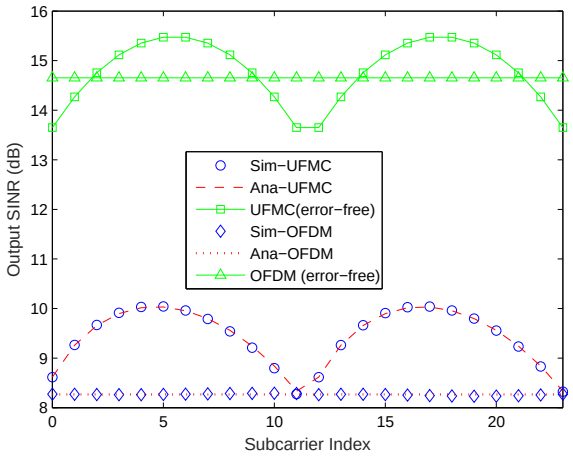

Fig. 3. Output SINR versus to subcarrier for both interference-free and interference cases.

Amplitude Modulation) with normalized power $\rho^2_{sym} = 1$. For all simulations, we also use the interference-free case (i.e., no CFO, TO and sufficient CP length: $L_{CP} = 160$) for both UFMC and OFDM systems as benchmarks.

The analytical results for desired signal $P_D(n)$ in equation (10) are compared with simulation results and shown in left-hand subplot of Fig. 2 with CFO and TO being $\epsilon = 0.1$ and $\tau = 85$ samples, respectively. Note that only the first two subbands (subcarrier index from 0 to 23) are shown. From Fig. 2, all of the analytical results concur with the simulated ones, which shows the effectiveness and accuracy of the signal model derivations. In both ideal and non-ideal cases, the UFMC system shows frequency selectivity over each subband. The analytical results for ICI and ISI given in equation (10) and simulation results are shown in right-hand subplot of Fig. 2. Again, the simulated and analytical results match to each other nearly perfectly on all accounts. In addition, the UFMC system suppressed the ISI to a lower level than the OFDM system in all subcarriers.

The analytical (based on equation (13)) and simulated output SINR for both UFMC and OFDM systems are shown in Fig. 3 with input SNR = 15 dB. In interference-free case, the UFMC system shows large SINR variation along the subcarriers, while the OFDM system shows a flat line. The UFMC system outperforms the OFDM system only in some subcarriers. However, with transceiver imperfections, the UFMC system outperforms the OFDM system in every single subcarrier. This proves that the subband filter in UFMC system can improve the performance in comparison to OFDM system.

Fig. 4 examines the effectiveness of the derived interference and desired signal power in (10), (11) and (12) in terms of Viterbi coded BER with coding rate being 1/2. Note that the low-complexity maximum log likelihood ratio (LLR) based algorithm is used in the simulation by assuming the interference-plus-noise having a Gaussian distribution [13]. We use two set of parameters, low level interference with $\epsilon_L = 0.03$; $\tau_L = 68$ samples, and a high level interference as $\epsilon_H = 0.06$; $\tau_H = 136$ samples. In ideal cases, Fig. 4 shows that the OFDM outperforms UFMC system by a small margin due to the filter frequency selectivity. However, in the presence of CFO and TO, the proposed UFMC system shows its advantage over the OFDM and original UFMC systems [1]

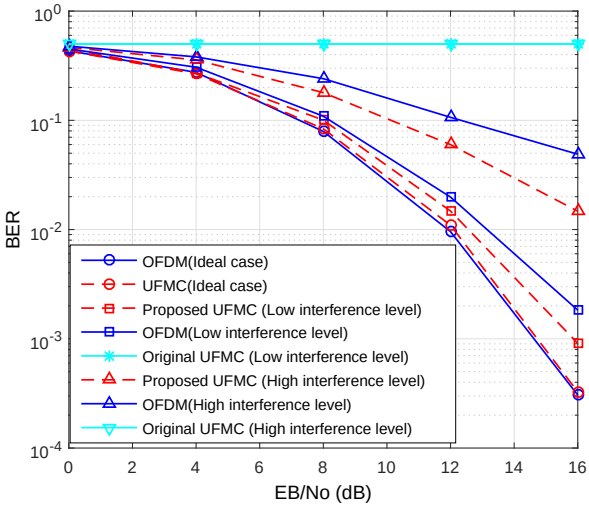

Fig. 4. Turbo coded BER performance versus E_b/N_0.

by suppressing interference effectively.

V. Conclusions

The CP-UFMC system has been proposed and analyzed in the absence of transceiver imperfections. The conditions for interference-free one-tap equalization and corresponding signal model have been derived. The model is extended to the scenarios of transceiver imperfections and insufficient CP length. The analytical expressions for desired signal, ICI and ISI are derived. Based on the analysis, new channel equalization algorithms are proposed. Our theoretical analysis results have been validated by simulations. The analytical framework developed in this paper provides a valuable reference for the design and development of practical UFMC systems.

Acknowledgement

The author would like to acknowledge the support of the University of Surrey 5GIC (http://www.surrey.ac.uk/5gic) members for this work.

REFERENCES

[1] 5GNOW, "D3.2: 5G waveform candidate selection," Tech. Rep., 2014.

[2] G. Wunder, P. Jung, and etc., "5GNOW: non-orthogonal, asynchronous waveforms for future mobile applications," *IEEE Communications Magazine*, vol. 52, no. 2, pp. 97–105, February 2014.

[3] Y. Chen, F. Schaich, and T. Wild, "Multiple access and waveforms for 5G: IDMA and universal filtered multi-carrier," in *IEEE Vehicular Technology Conference (VTC Spring)*, 2014, pp. 1–5.

[4] L. Zhang, A. Ijaz, P. Xiao, A. Quddus, and R. Tafazolli, "Single-rate and multi-rate multi-service systems for next generation and beyond communications," in *IEEE Personal, Indoor and Mobile Radio Communications (PIMRC)*, Sep. 2016, pp. 1–6.

[5] B. Farhang-Boroujeny, "OFDM versus filter bank multicarrier," *IEEE Signal Processing Magazine*, vol. 28, no. 3, pp. 92–112, May 2011.

[6] D. Chen, D. Qu, T. Jiang, and Y. He, "Prototype filter optimization to minimize stopband energy with NPR constraint for filter bank multicarrier modulation systems," *IEEE Transactions on Signal Processing*, vol. 61, no. 1, pp. 159–169, Jan 2013.

[7] D. Chen, X. G. Xia, T. Jiang, and X. Gao, "Properties and power spectral densities of CP based OQAM-OFDM systems," *IEEE Transactions on Signal Processing*, vol. 63, no. 14, pp. 3561–3575, July 2015.

[8] D. Noguet, M. Gautier, and V. Berg, "Advances in opportunistic radio technologies for TVWS," *EURASIP Journal on Wireless Communications and Networking*, vol. 2011, no. 1, pp. 1–12, 2011.

[9] A. Ijaz, L. Zhang, M. Grau, A. Mohamed, S. Vural, A. U. Quddus, M. A. Imran, C. Foh, and R. Tafazolli, "Enabling massive IoT in 5G and beyond systems: Phy radio frame design considerations," *IEEE Access*, 2016.

[10] X. Zhang, M. Jia, L. Chen, J. Ma, and J. Qiu, "Filtered-OFDM - enabler for flexible waveform in the 5th generation cellular networks," in *2015 IEEE Global Communications Conference (GLOBECOM)*, Dec 2015, pp. 1–6.

[11] H. Steendam and M. Moeneclaey, "Analysis and optimization of the performance of OFDM on frequency-selective time-selective fading channels," *IEEE Transactions on Communications*, vol. 47, no. 12, pp. 1811–1819, 1999.

[12] Y. Huang and B. D. Rao, "Awareness of channel statistics for slow cyclic prefix adaptation in an OFDMA system," *IEEE Wireless Communications Letters*, vol. 1, no. 4, pp. 332–335, 2012.

[13] X. Wang, T. Wild, F. Schaich, and A. Fonseca dos Santos, "Universal filtered multi-carrier with leakage-based filter optimization," in *European Wireless Conference*, 2014, pp. 1–5.

[14] X. Wang, T. Wild, and F. Schaich, "Filter optimization for carrier-frequency-and timing-offset in universal filtered multi-carrier systems," in *IEEE Vehicular Technology Conference (VTC Spring)*, 2015, pp. 1–6.